Carbon Nanotubes Dispersed in Aqueous Solution by Ruthenium(II) Polypyridyl Complexes

Kewei Huang,[a,†] Avishek Saha,[a,b,†] Konstantin Dirian,[b] Chengmin Jiang,[a] Edmund P. Chu,[a] James M. Tour,[a,c] Dirk M. Guldi,[b,*] Angel A. Martí[a,c,d,*]

[a]Department of Chemistry, Rice University, Houston, TX, 77005 (USA). [b]Department of Chemistry and Pharmacy and Interdisciplinary Center for Molecular Materials (ICMM), Friedrich-Alexander-Universität Erlangen-Nürnberg, Egerlandstraße 3, 91058 Erlangen, Germany. [c]Department of Materials Science & Nanoengineering, and [d]Department of Bioengineering, Rice University, Houston, TX, 77005 (USA).

Supporting Information

Table of contents

1. Characterization data

2. Time-resolved photoluminescence, Transient Absorption and Spectroelectrochemical data

3. Appendix 1. FRET efficiency for the couple **RuPy 1** and (6,5) SWCNTs.

1. Characterization data

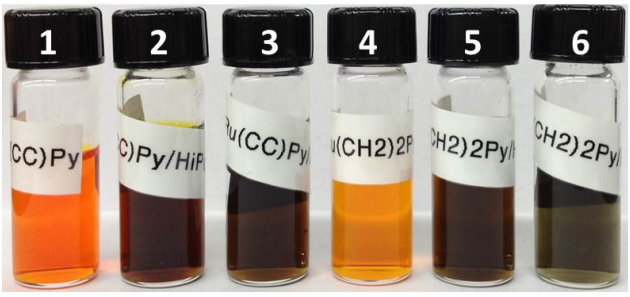

Figure S1. 1mg/ml **RuPy1** and **RuPy2** aqueous solutions and dispersions with SWNCTs. (1) 1mg/ml **RuPy1** in water solution; (2) 1mg/ml **RuPy1** with 1mg/mL HiPco SWCNTs in water solution before dialysis; (3) 1mg/ml **RuPy1** and 1mg/mL HiPco SWCNTs in water solution after dialysis for 16 hours; (4) 1mg/ml **RuPy2** in water solution; (5) 1

mg/ml **RuPy2** and 1mg/mL HiPco SWCNTs in water solution before dialysis; (6) 1mg/ml **RuPy2** and 1mg/mL HiPco SWCNTs in water solution after dialysis for 16 hours.

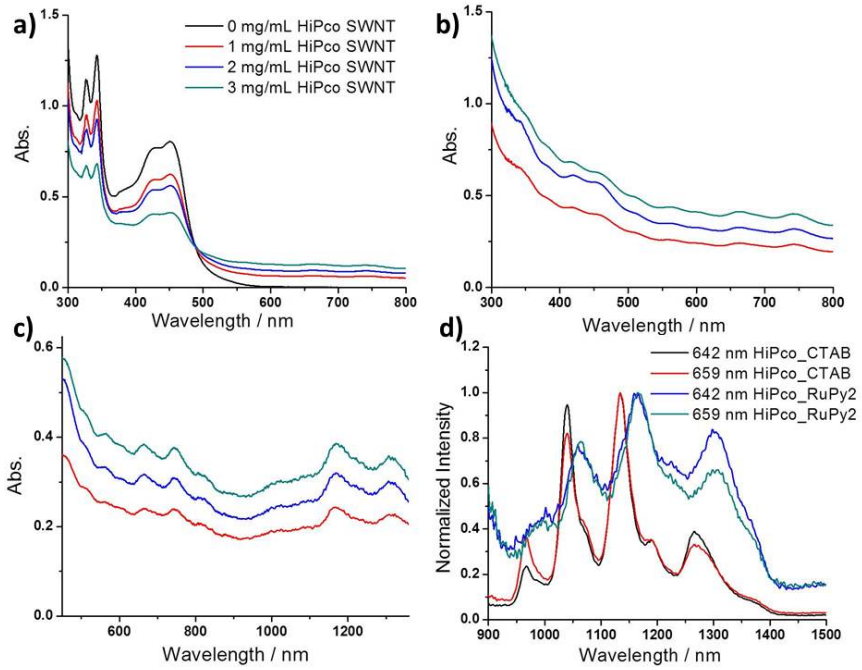

Figure S2. UV-Vis absorption spectra of **RuPy2** and HiPco SWCNT composites in aqueous solution before (a) and after (b) dialysis for 16 hours using nominal 2000 MW membrane. Dispersion solutions were prepared by 1mg/mL **RuPy2** with initial concentration of HiPco 0 mg/mL (black line), 1 mg/mL (red spectra), 2 mg/mL (blue spectra) and 3 mg/mL (cyan spectra), HiPco SWCNTs respectively (20x dilution for (a) and 5X dilution for (b) before taking the spectra); c) Visible-NIR absorption spectra of **RuPy2** and HiPco SWCNT composites in aqueous solution (5x dilution before taking the spectra). d) Normalized NIR-photoluminescence spectra of HiPco SWCNTs dispersed using **RuPy2** aqueous solution and CTAB surfactants.

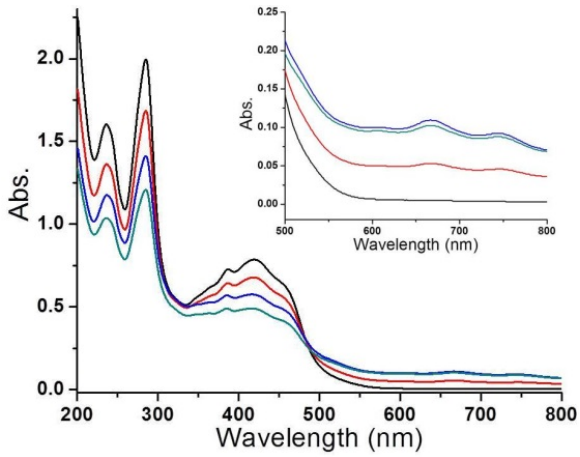

Figure S3. UV-Vis absorption spectra of **RuPy1** and CoMoCat SWCNTs composites in aqueous solution. Dispersion were prepared by using 1mg/mL **RuPy1** with initial concentration of 0 (black spectra), 1mg/mL (red spectra), 2mg/mL (blue spectra) and 3mg/mL (cyan spectra), CoMoCat SWCNTs respectively. All the solutions were diluted to 2.5% before taking the spectra.

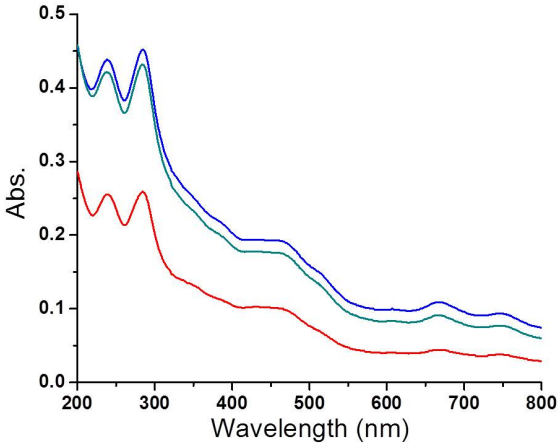

Figure S4. UV-Vis absorption spectra of **RuPy1** and CoMoCat SWCNTs composites in aqueous solution after dialysis for 16 hours using nominal 2000 MW membrane. Dispersions were prepared by using 1mg/mL **RuPy1** with initial amounts of 1 mg/mL (red spectra), 2 mg/mL (blue spectra) and 3 mg/mL (cyan spectra), of CoMoCat SWCNTs respectively. All the solutions were diluted to 2.5% before taking the spectra.

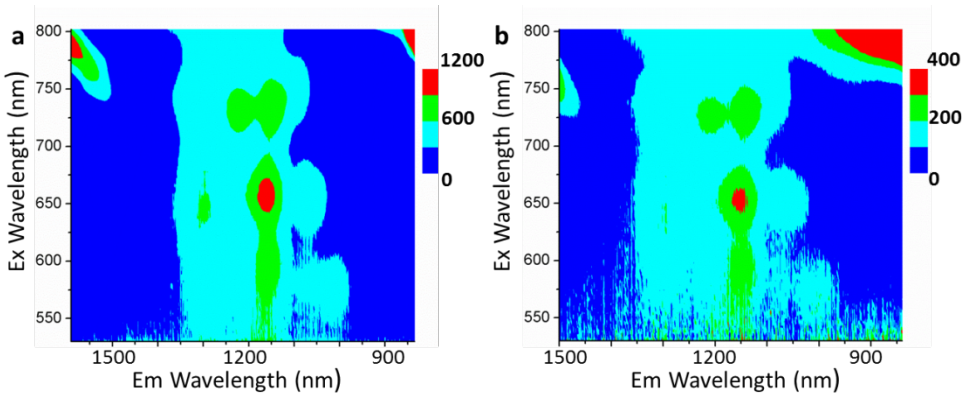

Figure S5. 3D steady-state photoluminescence spectra of (a) **RuPy1**/HiPco SWCNTs , (b) **RuPy2**/ HiPco SWCNTs in D_2O.

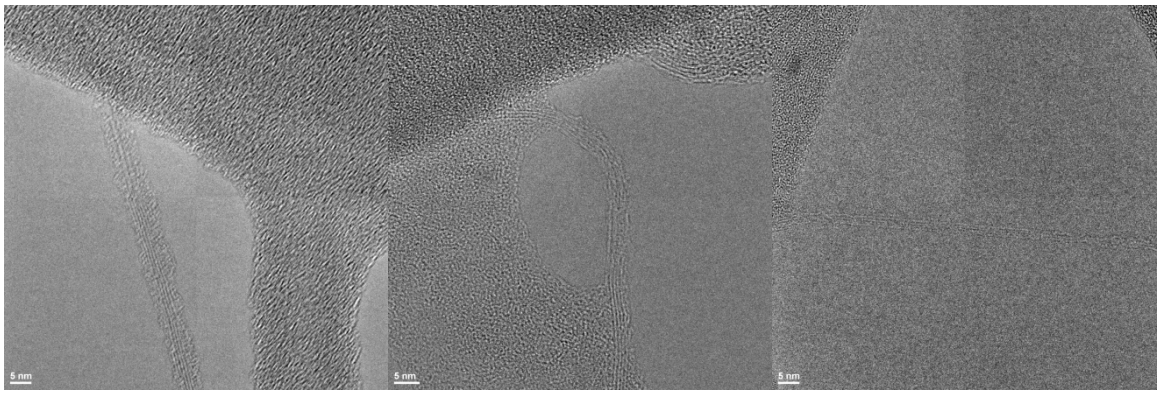

Figure S6. Representative TEM images of HiPco SWCNTs dispersed in **RuPy1** aqueous solution.

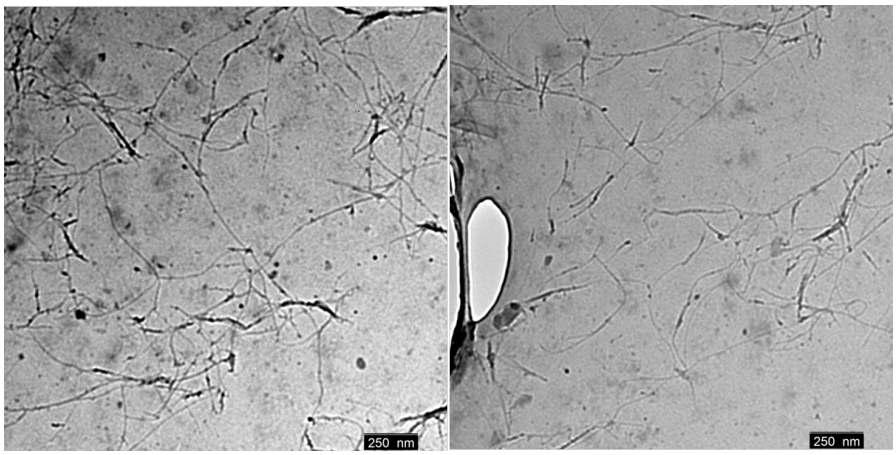

Figure S7. Representative TEM images of HiPco SWCNTs dispersed in **RuPy2** aqueous solution.

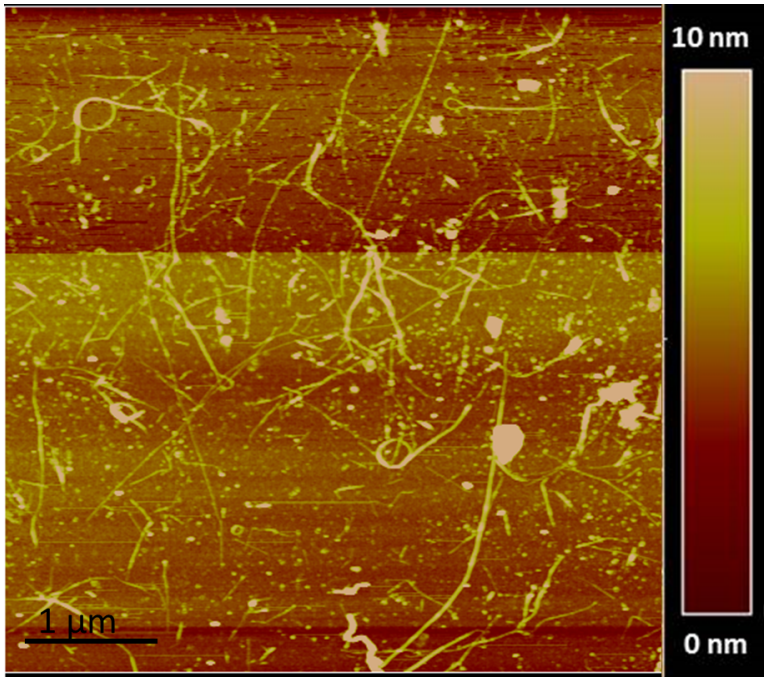

Figure S8. Representative AFM images of CoMoCat SWCNTs dispersed in **RuPy1** aqueous solution.

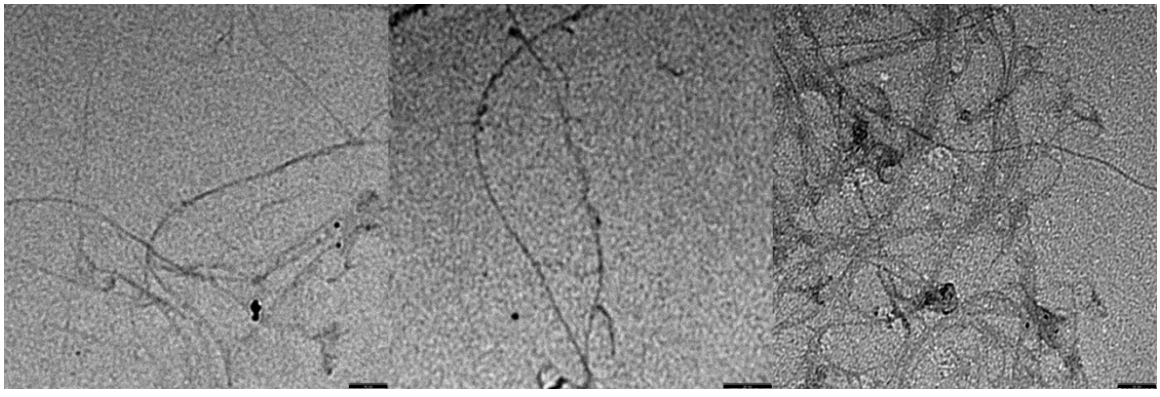

Figure S9. Representative TEM images of CoMoCat SWCNTs dispersed in **RuPy1** aqueous solution.

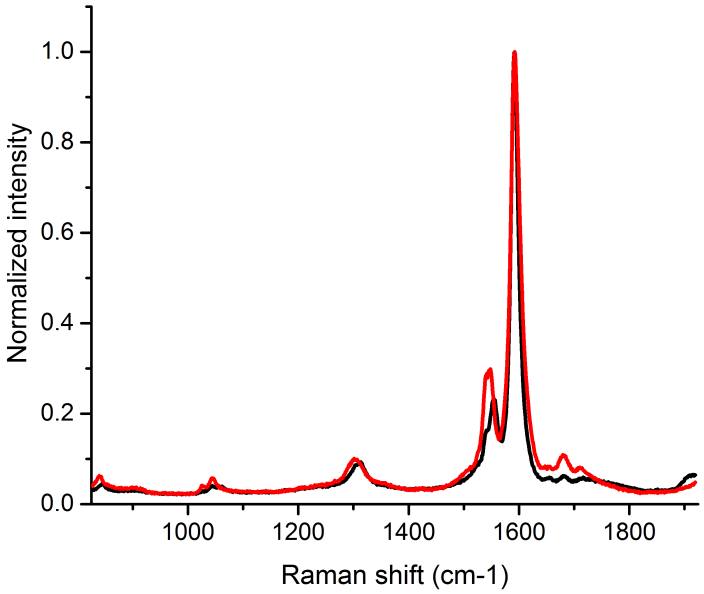

Figure S10. (a) Representative Raman spectra of **RuPy1**/HiPco SWCNTs (black spectrum) and **RuPy1**/CoMoCat SWCNTs (red spectrum) on silicon wafer. Spectra were taken upon 633 nm excitation.

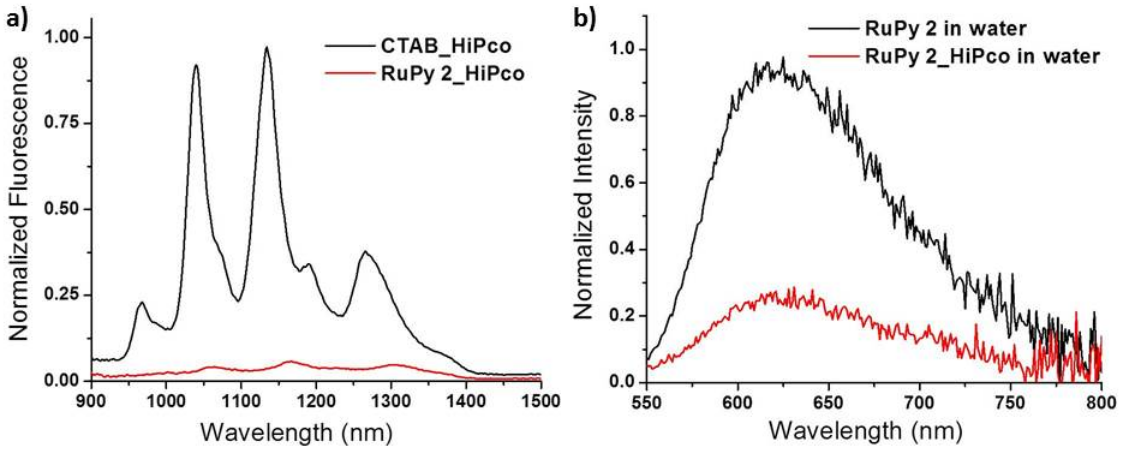

Figure S11. (a) The NIR photoluminescence of CTAB/HiPco SWCNTs (black line) and **RuPy2**/HiPco SWCNTs (red line) in aqueous solution (same concentration of HiPco in water, λ_{ex} = 642 nm); (b) The steady-state photoluminescence of **RuPy2** (black line), **RuPy2**/HiPco SWCNTs (red line) in aqueous solution (same concentration of **RuPy2** in water, λ_{ex} = 420 nm).

2. Time-resolved photoluminescence, Transient Absorption and Spectroelectrochemical data

Table S1. Photophysical properties of **RuPy1** and **RuPy2** complexes.

	λ_{abs}/nm	λ_{em}/nm	$\varepsilon/M^{-1}cm^{-1}$	τ/μs
RuPy1	419	628, 679, 744	33407	665.1[a]
RuPy2	452	616	16009	12.23[b]

a. Results were obtained in deaerated aqueous solution using μF 920H lamp with excitation at 420 nm and un-Cooled Blue as detector for **RuPy1.** Average lifetime, lifetime distributions of **RuPy1**: 734.6 μs (90.2%), 38.6μs (6.6%), 1.8 μs (3.2%).

b. Results was obtained in deaerated aqueous solution using a 440 nm picosecond pulse diode laser and a high speed red detector for **RuPy2**. Average lifetime, lifetime distributions of **RuPy2**: 12.9 μs (94.9%), 1.1 μs (5.1%).

Table S2. Photoluminescence lifetime of 1mg/mL **RuPy1** complexes with different concentration of HiPco SWCNTs in deaerated water solution before and after dialysis.

	Lifetime/μs	
Initial HiPco Conc.	Before Dialyais	After Dialysis
0 mg/mL	665.1 (average)	
	734.6 (90.2%) 38.6 (6.6%) 1.8 (3.2%)	
1 mg/mL	615.9 (average)	532.6 (average)
	665.6 (92.2%) 37.8 (6.1%) 1.9 (1.7%)	605.4 (87.8%) 12.9 (5.7%) 1.3 (6.5%)
2 mg/mL	760.7 (average)	382.8 (average)
	826.7 (91.7%) 42.5 (7.0%) 2.0 (1.3%)	442.1 (86.3%) 16.8 (5.0%) 1.8 (8.7%)
3 mg/mL	792.6 (average)	513.7 (average)
	870.9 (90.6%) 44.8 (8.2%) 2.4 (1.2%)	599.3 (85.5%) 13.5 (7.1%) 1.4 (7.4%)

Table S3. Lifetime of ground state bleaching of - HiPco and CoMoCat SWCNTs (in NIR region) dispersed by CTAB, **RuPy1**, and **RuPy2** in deaerated D_2O, from femto-second pump probe experiments (percentage of each component shown in parenthesis).

	Wavelength (nm)	τ_1 (ps)	τ_2 (ps)	τ_3 (ps)
CTAB/HiPco	989	3.5 (5.4%)	15.4 (15.6%)	166.1 (79.0%)
	1135	1.7 (6.4%)	23.8 (22.5%)	142.5 (71.1%)
CTAB/CoMoCat	993	2.2 (6.8%)	26.1 (19.2%)	174.9 (74.0%)
	1149	3.1 (12.6%)	45.5 (49.5%)	170.5 (37.9%)
RuPy1/HiPco	1000	2.3 (12.5%)	25.3 (27.1%)	136.1 (60.4%)
	1149	2.6 (12.1%)	36.4 (39.1%)	169.6 (48.8%)
RuPy2/HiPco	1000	2.3 (45.3%)	29.8 (36.1%)	102.0 (18.6%)
	1149	3.8 (19.1%)	36.1 (54.1%)	81.9 (26.8%)
RuPy1/CoMoCat	1010	2.4 (13.5%)	18.7 (21.3%)	136.5 (65.2%)
	1149	2.6 (24.9%)	44.3 (75.1%)	-
RuPy2/CoMoCat	1010	2.4 (19.6%)	17.1 (29.3%)	95.6 (51.1%)
	1149	2.0 (25.6%)	44.1 (74.4%)	-

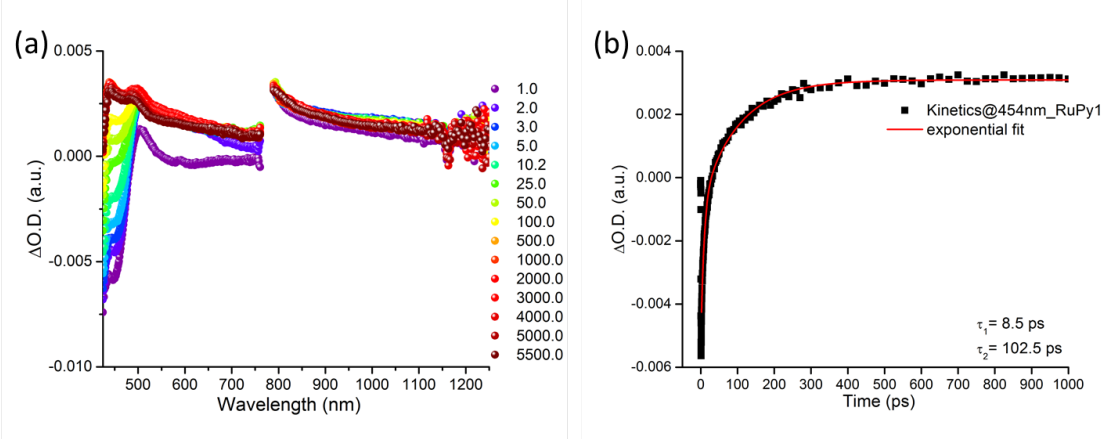

Figure S12. Differential absorption spectra (visible and infrared) obtained upon femtosecond pump probe experiments (387 nm) of (a) **RuPy1** in D_2O with time delays between 1 and 5500 ps, (b) Time absorption profile of the spectra shown in (a) at 454 nm. The recovery of the MLCT is accompanied with the formation of a positive transient (likely pyrene triplet state), which decay with a lifetime longer than the resolution of this experiment.

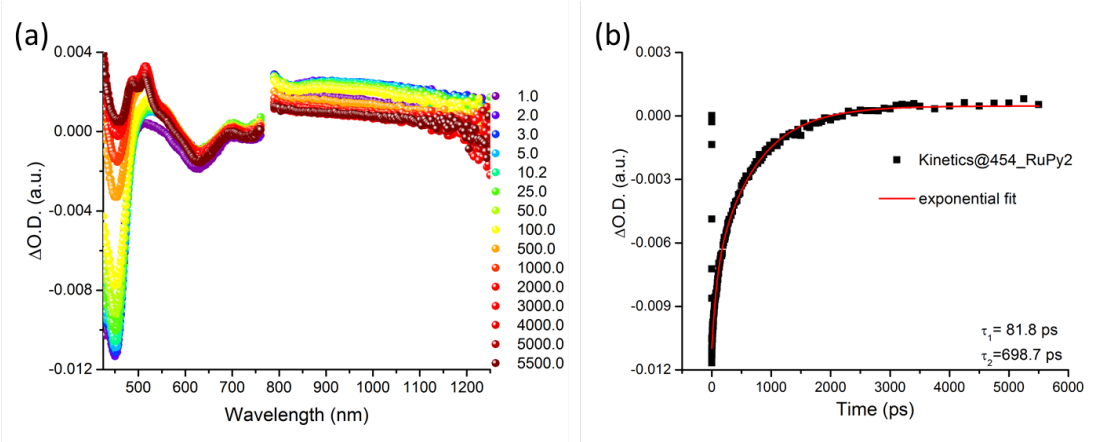

Figure S13. Differential absorption spectra (visible and infrared) obtained upon femtosecond pump probe experiments (387 nm) of (a) **RuPy2** in D_2O with time delays between 1 and 5500 ps, (b) Time absorption profile of the spectra shown in (a) at 454 nm. The recovery of the MLCT is accompanied with the formation of a positive transient (likely pyrene triplet state), which decay with a lifetime longer than the resolution of this experiment.

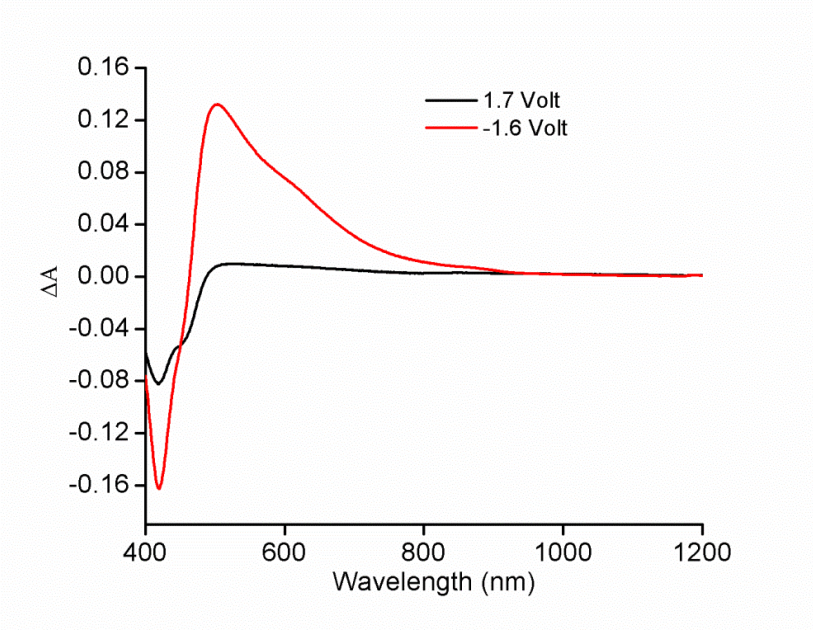

Figure S14. Differential absorption changes upon oxidation (black spectrum) and reduction (red spectrum) of **RuPy 1** in acetonitrile (0.2 M tetra-n-butylammonium hexafluorophosphate supporting electrolyte, potentials with regards to Ag wire).

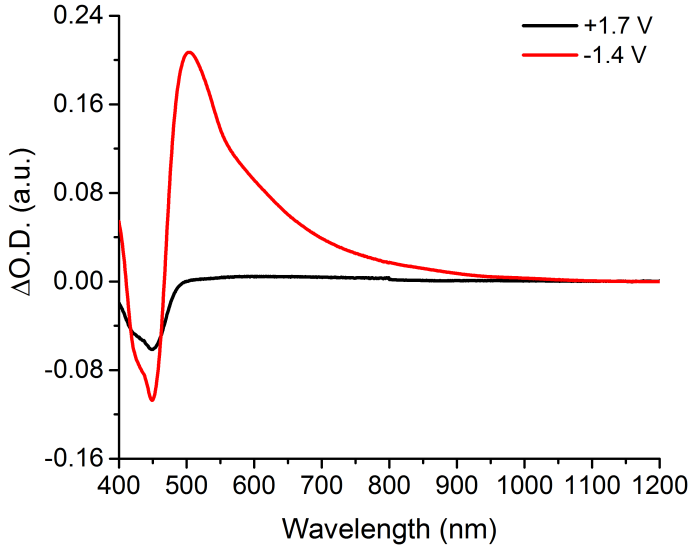

Figure S15. Differential absorption changes upon oxidation (black spectrum) and reduction (red spectrum) of **RuPy 2** in acetonitrile (0.2 M tetra-n-butylammonium hexafluorophosphate supporting electrolyte, potentials with regards to Ag wire).

Appendix 1. FRET efficiency for the couple **RuPy 1** and (6,5) SWCNTs.

To answer the question of whether quenching by FRET is possible, the rate of FRET and its efficiency can be calculated. This can be done by making some assumptions about our system. FRET rate constant can be calculated from:

$$k_{FRET}(r) = \frac{1}{\tau_D}\left(\frac{R_0}{r}\right)^6 \qquad (1)$$

where τ_D is the donor's lifetime, r is the distance between the donor and acceptor and R_0 is given by:

$$R_0^6 = \frac{9000(\ln 10)\kappa^2\phi J}{128\pi^5\eta^4 N_{Av}} \qquad (2)$$

R_0 is the Förster distance (the distance at which half of the donor excitation is transferred to the acceptor), κ^2 is the orientation factor (usually 2/3 for free molecules in solution), ϕ is the quantum yield of the donor, J is the spectral overlap constant, which describes the overlap between the donor emission spectrum and the acceptor absorption spectrum, N_{Av} is the Avogadro's number and η is the refractive index of the medium (~1.3).

Likewise, FRET efficiency can be calculated by:

$$E = \frac{R_0^6}{R_0^6 + r^6}$$

Thus, first we need to estimate the distance between **RuPy1** and the CNT, in this case a (6,5) CoMoCat SWCNT. Since the Ruthenium polypyridine part of the molecule has a charge of +2, it is reasonable to think that it will try to stay as retired from the hydrophobic surface of the carbon nanotube as possible. Also, we can assume as well that the hydrophobic pyrene group would try to have most of its surface in contact with the walls of SWCNTs. Therefore, if we put pyrene in van der Waals contact with SWCNTs, with the long axis of the molecule running along the carbon nanotube length, we get Figure A. The distance from the ruthenium polypyridyl complex and the center of the SWCNT is about 1.25 nm.

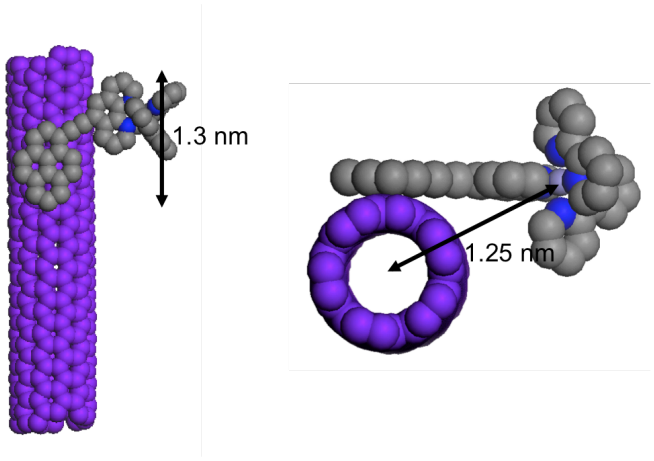

Figure S16. Structural model of the interaction between **RuPy1** and a (6,5) SWNCT.

The calculated lifetime of **RuPy1** is 665 μs. If we calculate R_0, then the rate and efficiency of FRET can be calculated at different distances. Our experiments show that the quantum yield of **RuPy1** is nitrogen purged acetonitrile is 0.027 and the refractive index of the medium was 1.3. To calculate J we need to have an idea of the extinction coefficient of SWCNTs. Hertel et al. calculated an extinction coefficient for the S_2 transition of (6,5) SWCNTs (band at ca. 991 nm) of 4400 M^{-1} cm^{-1} per carbon atom (Schöppler, F., Mann, C.; Hain, T. C.; Neubauer, F. M.; Privitera, G.; Bonaccorso, F.; Chu, D.; Ferrari, A. C.; Hertel, T. Molar Extinction Coefficient of Single-Wall Carbon Nanotubes *J. Phys. Chem. C*, **2011**, *115*, 14682-14686). From Figure S16, we can estimate that the projection of RuPy1 on the SWCNTs is about 1.3 nm. Therefore, if a (6,5) carbon nanotube has 88 carbons per nm, there are 114 C atoms per **RuPy1** length. If FRET is going to occur, it is reasonable to assume that it will occur to these carbon atoms close to the ruthenium center rather that carbon atoms farther away. With this information, we calculated an extinction coefficient for the 991 nm transition of (6,5) carbon nanotubes of 501600 $M^{-1}s^{-1.}$ The calculation of R_0 is done by normalizing the value of the 991 nm transition to this value and using the spectrum to calculate the overlap integral (*J*). R_0 (51.8 Å) and the rate and efficiency of FRET were calculated using FRETView (Stevens, N.; Dyer, J.; Martí, A. A.; Solomon, M.; Jockusch, S.; Turro, N. J. FRETView: a computer program to simplify the process of obtaining fluorescence resonance energy

transfer parameters, *Photochem. Photobiol. Sci.* **2007**, *6*, 909-911). The results are shown in table 1.

Table S4. FRET parameters for the interaction of **RuPy 1** and (6,5) SWCNTs.

r (Å)	E	k_{FRET} (s^{-1})	$\tau_{acceptor}$
8	1	1.10E+08	9.04 ns
9	1	5.50E+07	18.27 ns
10	1	2.90E+07	34.4 ns
11	1	1.60E+07	60.96 ns
12	1	9.70E+06	102.78 ns
13	1	6.00E+06	166.12 ns
14	1	3.90E+06	259.11 ns
15	0.999	2.60E+06	391.89 ns
16	0.999	1.70E+06	577 ns
17	0.999	1.20E+06	829.84 ns
18	0.998	8.50E+05	1.17 us
19	0.998	6.20E+05	1.62 us
20	0.997	4.50E+05	2.2 us
21	0.996	3.40E+05	2.94 us
22	0.994	2.60E+05	3.88 us
23	0.992	2.00E+05	5.06 us
24	0.99	1.50E+05	6.51 us
25	0.988	1.20E+05	8.3 us
26	0.984	9.40E+04	10.47 us
27	0.98	7.50E+04	13.07 us
28	0.976	6.00E+04	16.18 us

29	0.97	4.90E+04	19.86 us
30	0.964	4.00E+04	24.18 us
31	0.956	3.30E+04	29.21 us
32	0.947	2.70E+04	35.01 us
33	0.937	2.20E+04	41.67 us
34	0.926	1.90E+04	49.24 us
35	0.913	1.60E+04	57.78 us
36	0.899	1.30E+04	67.34 us
37	0.883	1.10E+04	77.96 us
38	0.865	9.60E+03	89.67 us
39	0.846	8.30E+03	102.46 us
40	0.825	7.10E+03	116.33 us
41	0.803	6.10E+03	131.24 us
42	0.779	5.30E+03	147.14 us
43	0.753	4.60E+03	163.95 us
44	0.727	4.00E+03	181.58 us
45	0.699	3.50E+03	199.91 us
46	0.671	3.10E+03	218.82 us
47	0.642	2.70E+03	238.16 us
48	0.612	2.40E+03	257.8 us
49	0.583	2.10E+03	277.58 us
50	0.553	1.90E+03	297.35 us
51	0.523	1.70E+03	316.99 us
52	0.494	1.50E+03	336.34 us
53	0.466	1.30E+03	355.31 us
54	0.438	1.20E+03	373.78 us
55	0.411	1.00E+03	391.66 us

56	0.385	9.40E+02	408.88 us
57	0.36	8.50E+02	425.39 us
58	0.337	7.60E+02	441.14 us
59	0.314	6.90E+02	456.1 us
60	0.293	6.20E+02	470.27 us
61	0.273	5.60E+02	483.65 us
62	0.254	5.10E+02	496.23 us
63	0.236	4.60E+02	508.03 us
64	0.219	4.20E+02	519.08 us
65	0.204	3.90E+02	529.39 us
66	0.189	3.50E+02	539.02 us
67	0.176	3.20E+02	547.97 us
68	0.163	2.90E+02	556.3 us
69	0.152	2.70E+02	564.03 us
70	0.141	2.50E+02	571.2 us
71	0.131	2.30E+02	577.85 us
72	0.122	2.10E+02	584.01 us
73	0.113	1.90E+02	589.72 us
74	0.105	1.80E+02	595 us
75	0.098	1.60E+02	599.89 us
76	0.091	1.50E+02	604.41 us
77	0.085	1.40E+02	608.59 us
78	0.079	1.30E+02	612.46 us
79	0.074	1.20E+02	616.04 us
80	0.069	1.10E+02	619.36 us